

Influence of Steel Mesh on Magnetic Proximity Detection Systems: An Experimental Study

Chenming Zhou^{*}, Bruce G. Whisner, Jacob L. Carr, and Justin Srednicki

Abstract—Proximity Detection Systems (PDSs) are used in the mining industry for protecting mine workers from striking, pinning, and crushing injuries when they work in close proximity to heavy machines such as continuous mining machines (CMMs). Currently all PDSs approved by the Mine Safety and Health Administration (MSHA) are magnetic field based systems which can be influenced by the presence of steel wire mesh that is commonly used for supporting roof and ribs in underground coal mines. In this paper, researchers at the National Institute for Occupational Safety and Health (NIOSH) characterized the influence of the mesh on the performance of magnetic PDSs by measuring the magnetic field difference around a CMM caused by the presence of the mesh. The results show that the magnetic fields are generally enhanced by the mesh which causes PDS detection zones to be increased correspondingly. It was discovered that the fields around the joints of two mesh sections have the greatest enhancement and thus deserve more attention. In addition, it was found that the presence of mesh can also cause a variation in the generator current. The experimental results show that the generator current variation and thus the magnetic field change caused by the mesh can be significant (on the order of ten) when the mesh is extremely close to the generator (e.g., less than 1 cm) and is negligible when mesh is relatively far (greater than 0.15 m). The findings in this paper can be used to develop guidelines and best practices to mitigate the influence of mesh on PDSs.

1. INTRODUCTION

The Mine Safety and Health Administration (MSHA) requires operators of underground coal mines to equip place-changing continuous mining machines (CMMs) with proximity detection systems (PDSs) to protect mine workers from striking, pinning and crushing injuries when they work around these heavy machines [1]. Although a variety of technologies can be implemented for proximity detection, the magnetic-field-based PDS that was originally developed at the National Institute for Occupational Safety and Health (NIOSH) has shown great effectiveness reducing proximity injuries in challenging mining environments and has been widely used in mines. Currently all MSHA-approved PDSs are magnetic-field-based systems.

As shown in Figure 1, a magnetic PDS typically includes two major components — the magnetic field generator and the Miner Wearable Component (MWC). Magnetic fields are generated by injecting a high electric current into a ferrite-rod antenna sealed in the generator. The magnetic field strength detected by an MWC varies with the distance between the MWC and the generator. In a typical PDS, multiple generators are mounted on different locations of the machine to establish two zones around the machine: the red zone (shutdown zone) and the yellow zone (warning zone) The yellow zone acts as the initial warning zone and signals a person with an MWC when he is getting too close to the equipment. The red zone is smaller, and functions as the shutdown zone that disables the machine when a person

Received 20 August 2019, Accepted 3 March 2020, Scheduled 6 March 2020

^{*} Corresponding author: Chenming Zhou (czhou@cdc.gov).

The authors are with the CDC NIOSH, Pittsburgh, PA, USA.

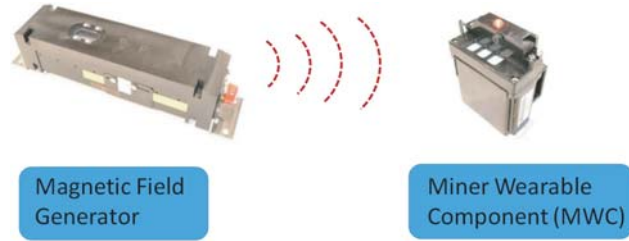


Figure 1. Two major components of a permissible magnetic PDS used in coal mines: the generator and the MWC.

wearing as MWC is detected in that zone. The relative location/zone of an MWC is determined based on the field strengths from different generators received by the MWC.

Ideally, for a PDS to work properly in the underground, the magnetic fields generated by the different generators should be stable and not vary with the environment, as the system would interpret any variation of the magnetic field as a result of the distance change between the machine and the miner wearing the MWC. In reality, however, this is not always the case since magnetic fields can be altered by a number of environmental factors such as the presence of steel wire mesh that has been widely used in underground coal mines for supporting roof and ribs. In this paper, the influence of mesh on the PDS performance is investigated and the magnetic field change caused by the mesh is measured.

Theoretically, mesh or other metallic objects can potentially influence the magnetic field radiated from a PDS generator through two mechanisms: antenna detuning and field shielding. The first effect, the antenna detuning effect caused by a nearby metallic object has been extensively investigated in the electromagnetic (EM) community, particularly for radio frequency identification (RFID) applications where radio frequency (RF) tags often need to be mounted on a metal structure [2–4]. It is found that the detuning effect caused by a metallic plate to a loop antenna can significantly degrade the performance of an RFID system by reducing the magnetic field received by the tag which leads to a decreased reading range of the system. It should be noted that research studies published in the literature are mainly based on high frequency loop antennas operated at 13.56 MHz with the antennas being the receiving unit. To our best knowledge, there has been no research conducted to characterize the influence of wire mesh to a transmitting rod antenna.

The second effect, the shielding effect, concerns the overall magnetic field distribution change caused by the presence of metallic objects. In this case, the mesh on roof and ribs shield the magnetic fields so that EM energy is confined inside the area formed by the mesh enclosure. As a result, the magnetic field distribution inside and outside of the mesh enclosure will be altered. It is known that the magnetic field outside the metallic enclosure will be attenuated which is the reason why a metallic enclosure is often used for shielding an interference source. What is concerned in this paper, however, is the field distribution change inside the enclosure. The problem of scattering of EM plane waves from a rectangular mesh screen has been theoretically treated by J. R. Wait and other researchers decades ago [5, 6]. Japanese researcher Yamaguchi found that adding mesh in a rectangular tunnel can enhance the EM field inside the tunnel and reduce the corresponding wave propagation loss [7, 8]. The reported studies on field distribution change caused by mesh screens are all theoretical studies and are at relatively high frequencies (\sim GHz). Experimental studies on field variation caused by mesh used in coal mines at frequencies below 1 MHz have not been reported.

In this paper, we investigate the influence of mesh on the performance of PDSs with an operating frequency of 73 kHz. Particularly, we designed experiments to quantify both of the antenna detuning and shielding effects caused by the mesh on the magnetic field generated from a permissible PDS.

2. MEASURING THE INFLUENCE OF MESH ON THE MAGNETIC FIELD OF PDSs

Measuring the antenna detuning caused by mesh: It is known that the magnetic field around a PDS generator is proportional to the current running through the antenna sealed inside the generator.

When a metallic object such as wire mesh is in close proximity to the antenna, the impedance of the antenna will be changed. As a result, the current on the antenna is changed, causing the magnetic field to change. A special experiment was designed to quantify the generator current change caused by the presence of mesh.

Figure 2 shows the experimental setup for measuring the generator current change caused by the wire mesh. During the experiment, one of the six generators of a commercial PDS was opened and a clamp-on current probe (HIOKI 3273-50) was placed inside the generator to monitor the current change. The current probe was connected to a digital oscilloscope (not shown in Figure 2) for displaying the current reading. A magnetic field loop antenna was also placed about 0.7 m behind the generator to monitor the magnetic field change during the experiment. The loop antenna was directly connected to a 16-bit analog to digital converter (ADC) (Model NI-9223, not shown in Figure 2) where the received voltage signals were sampled at a sampling rate of 1 million samples/second. A sliced piece of mesh (with a dimension of 0.71 m*1.52 m and a grid size of 0.1 m) was placed in front of the antenna. During the test, the distance between the generator and the mesh was varied and the corresponding magnetic field and current at different distances were recorded. It should be noted that during this test the field probe and the generator were all stationary and the mesh was moved either toward or away from the generator to vary the distance.

Measuring magnetic field distribution change caused by mesh: As shown in Figure 3, a wood supported simulated mesh entry $5.48 \times 3.05 \times 12.19 \text{ m}^3$ ($18 \times 10 \times 40 \text{ ft}^3$) was constructed to investigate

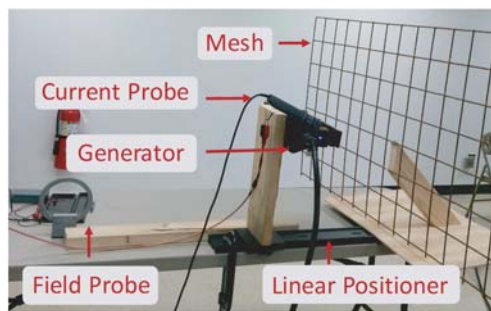


Figure 2. Experimental setup for measuring the generator current change caused by wire mesh.

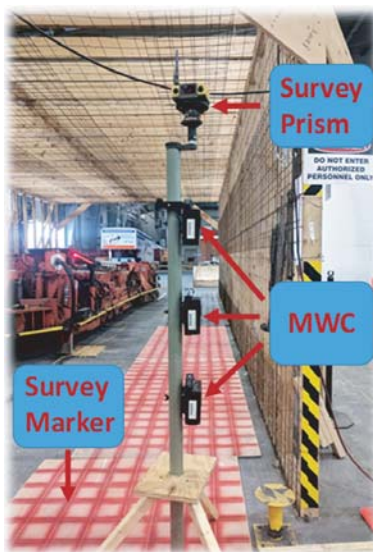


Figure 3. Experimental setup for surveying the magnetic field around a CMM parked inside a meshed area.

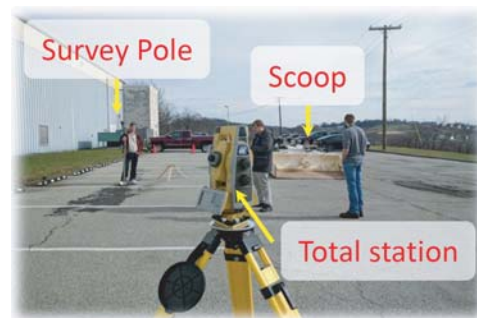


Figure 4. Experimental setup for surveying the red and yellow zones of a PDS installed on a scoop in an open environment.

the magnetic field distribution change caused by mesh. The steel mesh selected for this simulated mesh entry is one of the typical mesh types commonly seen in US underground coal mines. It has a square grid size of 0.15 m (0.5 ft) and a wire diameter of 4.8 mm (3/16 inch). Magnetic fields around a CMM machine were first surveyed in an open area without the presence of the mesh and then in the simulated meshed entry. To ensure that the measured field difference is caused by the mesh rather than a different distance between the MWC and the generator, the fields were surveyed at the same set of fixed locations relative to the CMM. To do this, some survey markers (shown in Figure 3) were carefully placed on the floor around the CMM and an optical total station system (TOPCON QS3A) was used to measure the coordinate of each marker. The measured coordinate was then translated to the coordinate of the CMM relative to the pivot point which is the center point of the CMM when it turns its direction.

The magnetic field at each survey marker around the CMM was measured using the intelligent PDS system [9, 10]. As shown in Figure 3, three MWCs are mounted at different heights (0.75 m, 1.05 m, and 1.35 m) on a survey pole. Those MWCs have an embedded three-axis ferrite loop antenna which converts the magnetic fields from the four generators to voltage signals. The converted voltage signals (i.e., magnetic fields) are then digitalized and wirelessly sent back to a controlling box installed on the CMM, through another radio link at around 900 MHz. A laptop is used to wirelessly read the magnetic field data received by each MWC from the controlling box through a LabVIEW program. As a result, on each position marker, a total of 12 magnetic field measurements are recorded which include the field readings for three MWCs from four generators.

Measuring the change on the size of the detection zones caused by mesh: Figure 4 shows the experimental setup for surveying the red and yellow zones of a PDS installed on a scoop in an open environment. The scoop (CAI 4880) used in this test is a rubber tired-, battery-powered equipment designed for cleaning runways and hauling supplies in underground coal mines. The survey pole used in this test is the same pole as shown in Figure 3, except that only one (instead of three) MWC is mounted on the pole at a height of 1.05 m. To find the boundary of the yellow zone, the survey pole was moved slowly toward the scoop, along a path perpendicular to the outline of the scoop, until the yellow zone alarm beeps. The 3D coordinates of the boundary location (i.e., the location of the survey pole) were then recorded by using the total station. This constitutes one sample point of the yellow zone boundary. The same process was repeated until the complete yellow zone boundary was identified and then the red zone boundary was surveyed in a similar manner. This boundary searching process was then repeated after the scoop was moved into the simulated mesh entry shown in Figure 3.

The measured coordinates are based on a coordinate system defined by the total station at the beginning of the measurement. Such coordinate system changes when the total station is moved which was the case when measuring the yellow and red zones in different environments. In order to compare the measured zones in different environments (i.e., with and without mesh), it is necessary to plot zones in the same coordinate system. To overcome the coordinate challenge, a machine-oriented coordinate system has been selected as the common coordinate system where the measured zone coordinates in different environments can be plotted and compared. As a result, a few fixed points on the scoop were selected as the reference points the coordinates of which were surveyed when the scoop was in different environments. These fixed points define the machine-oriented coordinate system.

3. RESULTS AND DISCUSSION

Generator current change caused by the mesh (the antenna detuning effect): Figure 5 shows the measured magnetic field and current when the mesh was placed at different distances from the PDS generator. For a better comparison, the measured magnetic field was normalized with respect to the maximal field and then was scaled to the maximum of the current. It is shown in Figure 5 that the magnetic field varies with the distance between the mesh and the generator, indicating that the presence of mesh influences the magnetic field of the generator. This influence is more significant when the mesh is closer to the generator. For example, when the mesh is located 1 cm from the generator, the magnetic field is reduced to about one tenth of the normal magnetic field value which was measured without the presence of the mesh. This normal magnetic field value was also found to be close to the value shown in Figure 5 for greater than 0.25 m. It can be observed in Figure 5 that the magnetic field change caused by the mesh is not significant when the mesh is located far (0.15 m or more) away from the generator.

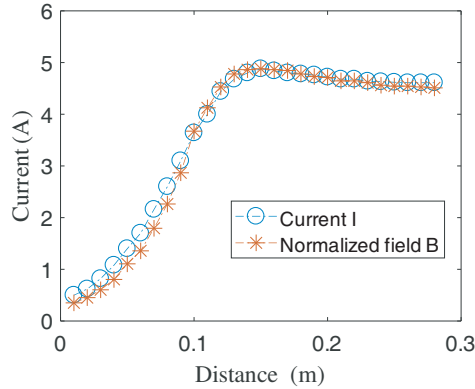


Figure 5. Measured current and normalized magnetic field change with respect to the distance between the generator and the mesh.

Additionally, a comparison between the magnetic field change and the current change shows that the two changes are highly correlated, indicating that the field change is mainly caused by the current change in the generator.

While it is generally expected that the magnetic field will be enhanced by metallic objects nearby, it is interesting to note that in this case the magnetic field is reduced rather than being enhanced when the mesh is close to the generator. The reason is that the antenna of the generator has been tuned (by a sliding metal piece called a “shunt”) without the presence of the mesh. The presence of the mesh causes the antenna to be detuned and thus the magnetic field is reduced. We verified this hypothesis by removing the “shunt” from the antenna and then repeating the test. It was found that the magnetic field is significantly enhanced when the mesh is close to the generator.

It should be noted that this is the only test that was based on the obsolete six-generator system and all other tests reported in this paper were based on the NIOSH intelligent PDS system which has four generators. The reason for using this obsolete model for this particular test is that one of the generators needs to be opened in order to insert the current probe. Although the test was conducted based on the obsolete system, we expect that the associated results and findings can be applied to newer models.

Magnetic field distribution change caused by mesh (the shielding effect): Figure 6 shows a comparison of the surveyed points around the CMM for in-mesh and out-mesh scenarios. Each dot in Figure 6 represents a surveyed point and is plotted based on the coordinate relative to the pivot point of the CMM converted from the 3D coordinates recorded by the total station. The blue dots are plotted based on the translated coordinates when the CMM is in the open area (the out-mesh scenario) and the red dots are plotted based on the translated coordinates of surveyed points when the CMM is in

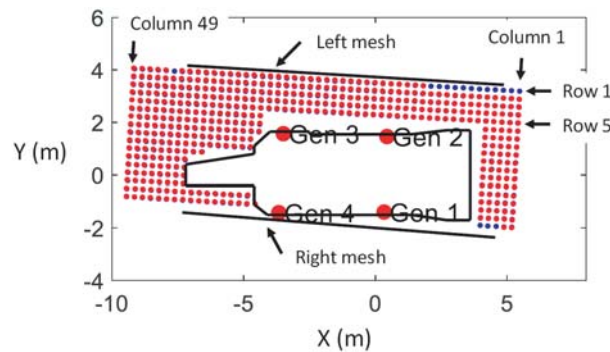


Figure 6. An illustration of the surveyed points around a CMM. Dots (with red dots for the in-mesh scenario and blue dots for the out-mesh scenario) are plotted based on the coordinates of the surveyed points measured by the total station. The grid size for surveyed points is 0.305 m (1 foot).

the meshed area (the in-mesh scenario) In addition, the location of the mesh, outline of the CMM, and the generators are all plotted based on the coordinates measured by the total station. It is shown in Figure 6 that the blue dots are largely overlapped with the red dots, indicating that survey markers were successfully placed at the same locations relative to the CMM for the in-mesh and out-mesh scenarios. Under this condition, fields surveyed at each location for the two scenarios can be compared and the difference can be attributed to the influence of mesh, since those fields are surveyed at the same location relative to the CMM There were a few locations where the survey prism was obstructed from the total station when the CMM was inside the meshed area. As a result, some of the locations in Figure 6 only have blue dots and the corresponding red dots are missing from the Figure This is the case, for example, from column 1 to column 12, at row 1. The grid size, i.e., the distance between two adjacent dots in Figure 6 is 0.305 m (one foot).

The CMM was parked close to the right mesh, with Gen 1 and Gen 4 located about 0.483 m (19 inches) and 0.229 m (9 inches) from the right mesh, respectively. According to our test result shown in Figure 5, the antenna detuning effect caused by the mesh at this distance was not significant. As illustrated in Figure 6, Row 1 is parallel to the left mesh with a distance of 63.5 mm (2.5 inches). To investigate the mesh proximity effect, an additional row, Row 0, was added to measure the magnetic field when the MWC is directly against the mesh with a “zero” distance. As shown in Figure 6, the red dots (i.e., surveyed positions) from column 3 to column 43 are in the meshed area.

Figure 7 shows how the magnetic field changes when an MWC is located at different distances to mesh, from row 5 to row 0. While the expected field reduction is observed from row 5 to row 0 due to the increased distance between the MWC and the generator, a few magnetic field peaks are shown in Figure 7 at rows 0, indicating that at some locations (e.g., column 13, row 0) the magnetic field is significantly higher than other locations, even though their locations are relatively far from the generator. A close look at those magnetic field peaks reveals that those peaks occur only when the MWC is close to the mesh (i.e., lower row numbers) and at the places where two mesh sections are cascaded. As an example, the embedded picture in the upper left corner of Figure 7 illustrates the mesh joints around column 13. For the simulated mesh entry we built, each mesh section is about 10 feet long so the mesh joints occur at columns 3 (starting point of the mesh coverage), 13, 23, 33, and 43 (end of mesh coverage), correlated with the locations of those magnetic field peaks. In other words, Figure 7 shows that there is strong magnetic field enhancement when MWCs are located around a mesh joint.

It can also be observed from Figure 7 that magnetic field peaks are not significant for rows 3, 4, and 5. As a result, one can conclude that the extreme magnetic field enhancement caused by mesh joints can be mitigated by keeping the MWC away (at least 2.25 feet) from the mesh joints. In addition to staying

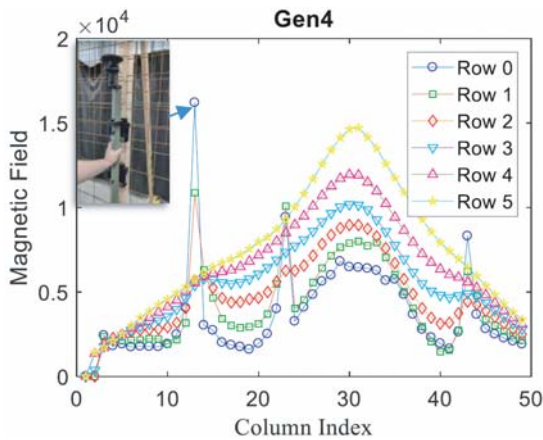


Figure 7. A comparison of the magnetic fields for different rows inside the meshed area. Row 0 is for the case where the MWC is directly against the left mesh. The locations for rows 1–5 are shown in Figure 6.

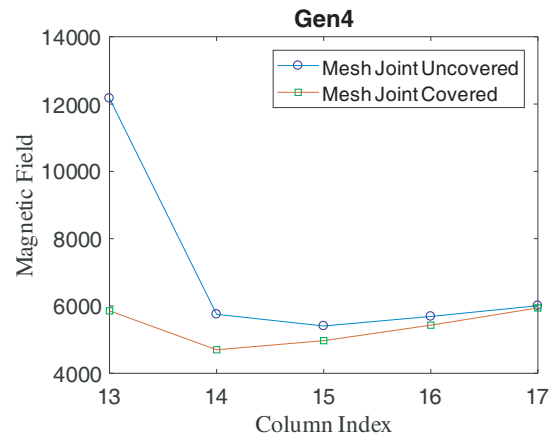


Figure 8. A comparison of the magnetic fields around column 13 for covered and uncovered mesh joint scenarios.

away from mesh joints, another strategy that might help alleviate the magnetic field enhancement effect caused by a mesh joint is to place an additional layer of mesh to cover the joint. To measure the effectiveness of the later alleviation method, we used a sliced mesh of $1.52 * 1.52 \text{ m}^2$ ($5 * 5 \text{ ft}^2$) to cover the mesh joint around column 13 where the magnetic field enhancement is shown to be the most significant. Figure 8 shows a comparison of the measured magnetic fields around column 13 for covered and uncovered mesh joint. It is clear from Figure 8 that the magnetic field around the mesh joint is reduced by about half when the joint is covered by another section of mesh.

Figure 9 shows a comparison of the magnetic field from Generator 4 for two different scenarios: with and without mesh, when the MWC is close to mesh (at row 1 shown in Figure 6). Again, the magnetic field enhancement due to mesh joint effect is apparent in Figure 9. It is also clear that the overall magnetic field distribution is changed due to the presence of the mesh. This change is not a uniform increase or decrease for different locations. Instead, the field, depending on the location of the MWC, increases around the mesh joints and decreases between the two adjacent joints. The green rectangular box in Figure 9 (starting from column 3 to column 43) represents meshed area for the in-mesh scenario.

The zero magnetic field (e.g., in magnetic fields shown in Figure 9) represents that the field at those locations is too low to enable the MWC to give a valid field reading. In this case, the magnetic field reading from the MWC stops updating itself, causing a system “frozen” incidence. It should be noted that system frozen incidences can also be caused by electromagnetic interferences as described in [11] for this particular PDS.

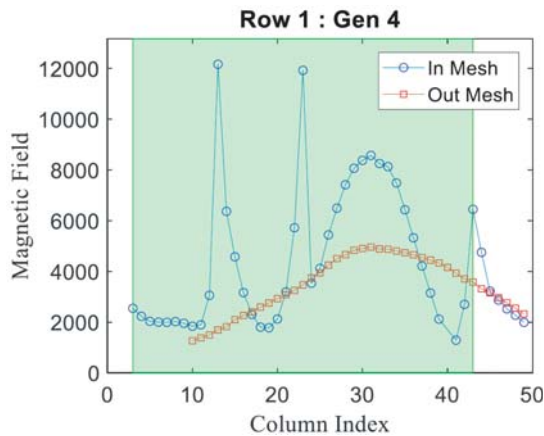


Figure 9. A comparison of the magnetic field for the in and out mesh scenarios when the MWC is close to the mesh. (Row 1).

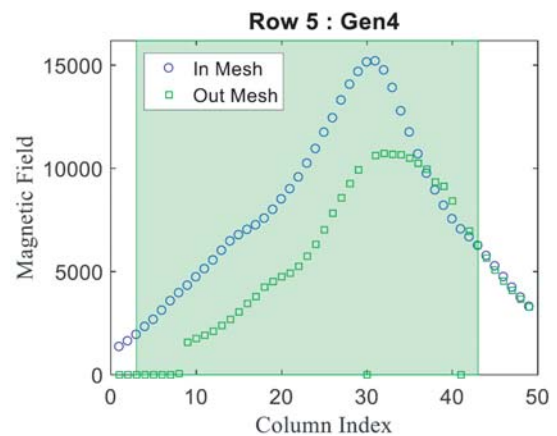


Figure 10. A comparison of the magnetic fields for in and out mesh scenarios when the MWC is relatively far from the mesh. (Row 5).

Similarly, Figure 10 shows the magnetic field comparison from the same generator (generator 4) for with and without mesh for row 5 where the MWC is located far from the mesh but relatively close to the generator as compared to row 1. For this case, the magnetic field distribution distortion caused by mesh joints is not obvious. Instead, the magnetic fields at different locations show a relatively more uniform increase in the meshed area. Again, the green box illustrates the mesh coverage.

Change on the yellow/red zone size caused by mesh: Figure 11 shows the measured yellow zone boundaries for different environments. The zone measured in open space is shown as yellow circles and the zone in the simulated mesh entry is shown as blue circles. As stated in the experimental setup section of the paper, the coordinates of those zone boundaries were originally measured under different coordinate systems. In Figure 11, those coordinates have been transformed to the machine-oriented coordinate system through coordinate transformation (i.e., coordinate translation and rotation). This was done in the data post-processing stage by using translation and rotation matrices. The pivot point of the scoop has been chosen as the origin of the new machine-oriented coordinate system. A reflector was permanently welded on the scoop to mark each reference point (including the origin) and is shown in yellow star in Figure 11. A comparison of the yellow zones shown in Figure 11 shows that the yellow zone in the simulated mesh entry is expanded about 2m as compared to the zone in open space. It

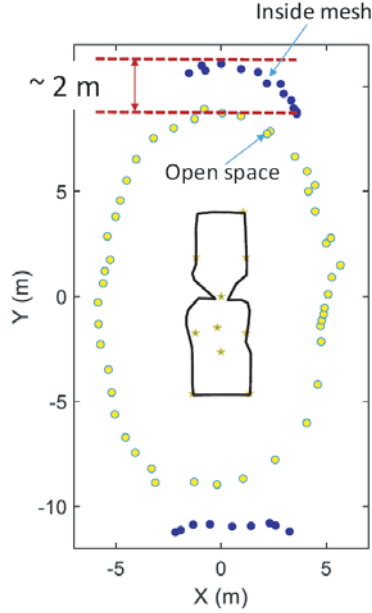


Figure 11. A comparison of the measured yellow zone boundary for in and out mesh scenarios.

should be noted that only two small portions of the yellow zone (rather than a complete zone) was surveyed when the scoop was inside the simulated mesh entry, due to the space restriction caused by the limited width of the simulated mesh entry. In addition, due to the limited length of the simulated mesh entry, a small part of the scoop had to stay outside of the meshed entry when the yellow zone was surveyed. For example, when the zone boundary on the front (bucket) end was surveyed, part of the back (battery) end of the machine stayed outside of the mesh. All four generators were always in the simulated mesh entry and are at least 15 cm distance away from ribs when the yellow zone was surveyed. The outline of the scoop in Figure 11 was plotted based on coordinates measured by the total station and represents the actual size of the machine.

Similarly to the yellow zone, it was observed that the size of the red zone also increases about 0.7 m when the scoop moved into the meshed entry. It should be noted that the measured changes on the size of the two zones, i.e., 2 m (for the yellow zone) and 0.7 m (for the red zone) are approximate results for this specific test only and the actual zone size change caused by mesh in different mines may vary, depending on many factors such as the dimensions of the entry and the transmitted power that the PDS generators are configured to.

4. CONCLUSIONS

The influences of mesh on the performance of a PDS, i.e., the antenna detuning effect and the shielding effect are experimentally characterized in this paper. It is found that the generator current and thus the magnetic field can be significantly changed (on the order of ten) when the generator is extremely close (~ 1 cm) to the mesh. This is due to the antenna detuning effect which can be mitigated by keeping the generator away from the mesh (e.g., with a distance greater than 0.15 m for the particular case studied). The fields generated by a PDS are found to be higher when the PDS is inside the simulated mesh entry as compared to the fields in open space, causing the corresponding yellow/red zones to be expanded. This field enhancement is most significant around joints of two mesh sections. The results in this paper can be used to develop guidelines and best practices on mitigating the influence of mesh on PDSs used in underground coal mines. For example, mine workers should be aware of the possible zone expansion when a machine enters into a meshed area and physically stay away from mesh when possible.

One of the limitations of the study is that the tests were conducted above the ground based on a simulated mesh entry without the presence of coal seam. The results, however, are expected to be applicable to the corresponding underground scenarios as the earth strata and coal seam have

relatively small influence on the magnetic field distribution, as demonstrated in a prior NIOSH research project [12]. In addition, to avoid the influence caused by the mesh on the PDS, miners might be required to reposition himself away from the mesh. This might affect the daily activities of those miners and machine operators and thus introduce new behavior changes that need to be further studied.

ACKNOWLEDGMENT

The authors would like to thank Jeff Yonkey and Nicholas Damiano for their help on the measurements. The authors would also like to thank Dr. Jingcheng Li for the valuable discussions.

5. DISCLAIMER

The findings and conclusions in this paper are those of the authors and do not necessarily represent the official position of the National Institute for Occupational Safety and Health, Centers for Disease Control and Prevention. Mention of any company or product does not constitute endorsement by NIOSH.

6. CONFLICT OF INTEREST

On behalf of all authors, the corresponding author states that there is no conflict of interest.

REFERENCES

1. *Proximity Detection Systems for Continuous Mining Machines in Underground Coal Mines*, MSHA, 2015.
2. Qing, X. and Z. N. Chen, "Proximity effects of metallic environments on high frequency RFID reader antenna: Study and applications," *IEEE Transactions on Antennas and Propagation*, Vol. 55, No. 11, 3105–3111, 2007.
3. Dobkin, D. M. and S. M. Weigand, "Environmental effects on RFID tag antennas," 135–138, 2005.
4. D'hoë, K. and V. Nieuwenhuyse, "Influence of different types of metal plates on a high frequency RFID loop antenna: Study and design," *Advances in Electrical and Computer Engineering*, Vol. 9, No. 2, 3–8, 2009.
5. Otteni, G., "Plane wave reflection from a rectangular-mesh ground screen," *IEEE Transactions on Antennas and Propagation*, Vol. 21, No. 6, 843–851, 1973.
6. Hill, D. A. and J. R. Wait, "Electromagnetic surface wave propagation over a bonded wire mesh," *IEEE Transactions on Electromagnetic Compatibility*, No. 1, 2–7, 1977.
7. Yamaguchi, Y., T. Honda, and M. Sengoku, "Reduction of wave propagation loss by mesh in rectangular tunnels," *IEEE Transactions on Electromagnetic Compatibility*, Vol. 37, No. 1, 88–93, 1995.
8. Yamaguchi, Y., T. Honda, M. Sengoku, S. Motooka, and T. Abe, "On the reduction of wave propagation loss in tunnels," *IEEE Transactions on Electromagnetic Compatibility*, Vol. 34, No. 2, 78–85, 1992.
9. Carr, J. L. and J. P. DuCarme, "Performance of an intelligent proximity detection system for continuous mining machines," *SME Annual Meeting*, 1–6, Denver, CO, 2013.
10. Carr, J. L., C. C. Jobes, and J. Li, "Development of a method to determine operator location using electromagnetic proximity detection," *2010 IEEE International Workshop on Robotic and Sensors Environments (ROSE)*, 51–56, Phoenix, AZ, 2010.
11. Noll, J., J. Ducarme, J. Li, R. J. Matetic, M. Reyes, J. Srednicki, and C. Zhou, "Electromagnetic interference with proximity detection systems," 2018.
12. Li, J., J. Carr, J. Waynert, and P. Kovalchik, "Environmental impact on the magnetic field distribution of a magnetic proximity detection system in an underground coal mine," *Journal of Electromagnetic Waves and Applications*, Vol. 27, No. 18, 2416–2429, 2013.